Naunyn-Schmiedeberg's Archives of Pharmacology (2018) 391:445–453
https://doi.org/10.1007/s00210-018-1474-8

ORIGINAL ARTICLE

Improved neuroprotective effect of resveratrol nanoparticles as evinced by abrogation of rotenone-induced behavioral deficits and oxidative and mitochondrial dysfunctions in rat model of Parkinson's disease

Suresh Palle[1] · Prasad Neerati[1]

Received: 8 October 2017 / Accepted: 24 January 2018 / Published online: 6 February 2018

Abstract

The objective of the present study was to evaluate the protective effect of resveratrol nanoparticles (NRSV) against rotenone-induced neurodegeneration in rats. NRSV were prepared by temperature-controlled antisolvent precipitation method and characterized for its particle size, shape, and dissolution properties. Moreover, NRSV effects compared with the free resveratrol (RSV). Animals were divided into four groups: (I) control, (II) rotenone (2 mg/kg s.c.), (III) RSV (40 mg/kg, p.o.) + rotenone, and (IV) NRSV (40 mg/kg, p.o.) + rotenone. Animals received treatments 30 min before rotenone administration for a period of 35 days. Behavioral quantifications were done using rota rod test and rearing behavior after 24 h of last dose. Animals were euthanized, and mid brains were isolated for the estimation of tricarboxylic acid cycle enzymes, oxidative measures (lipid peroxidation (LPO), glutathione (GSH), and catalase), and complex-I activity. In addition, histopathological studies were also performed. Our results showed that chronic rotenone treatment causes motor deficits, decreased rearing behavior, mitochondrial dysfunction, and oxidative stress. Furthermore, histological analysis demonstrated neuronal degeneration in rotenone-treated rats. An important finding of the present study was NRSV showed comparatively better efficacy than the RSV treatment in attenuating the rotenone-induced Parkinson's like behavioral alterations, biochemical and histological changes, oxidative stress, and mitochondrial dysfunction in rats.

Keywords Parkinson's disease · Resveratrol · Nanoparticles · Rotenone

Introduction

Parkinson's disease (PD) is a chronic neurodegenerative disorder, mainly causes motor impairments in the elderly population. A pathological hallmark of PD is increased oxidative stress and mitochondrial dysfunction, which may arise due to the selective inhibition of complex I activity (Hu et al. 2010; Tapias et al. 2014). Existing literature demonstrates that exposure to pesticides and environmental toxins can trigger oxidative damage and mitochondrial dysfunction (Supriya Swarnkar et al. 2011). Hence, abnormalities of mitochondrial energy metabolism may lead to alteration in oxidative homeostasis augmenting the formation of free radicals and development of many neurodegenerative disorders (Saravanan et al. 2005).

Rotenone (Fig. 1) is a naturally occurring, organic pesticide, derived from the plant roots of leguminosae family. It crosses blood-brain barrier easily and causes neurotoxicity by mitochondrial complex-I inhibition (Bueler 2009; Alam and Schmidt 2002). In rats, rotenone produces behavioral, neuropathological, and biochemical symptoms that resembles PD in humans (Betarbet et al. 2000).

Despite intensive advancement in research currently, the available therapies for PD only alleviate the symptoms and exhibit severe adverse effects, which preclude their long-term use (Wang et al. 2016). Therefore, developing new treatment modalities with improved biocompatibility and fewer side effects is necessary to ameliorate complications associated with PD. In this context, reduction of oxidative stress and mitochondrial dysfunction with specific antioxidants has been proven to be effective in the treatment of PD (Olanow et al. 2004). It has been reported that several exogenous herbal antioxidants derived from natural sources alleviate oxidative stress and improve mitochondrial function in rotenone-induced animal models of PD (Khurana and Gajbhiye 2013).

✉ Prasad Neerati
prasadneerati@gmail.com

[1] DMPK & Clinical Pharmacology Division, Department of Pharmacology, University College of Pharmaceutical Sciences, Kakatiya University, Warangal, TS 506002, India

Resveratrol (RSV) (Fig. 1) is a polyphenol belonging to the phytoalexin family, abundantly found in various plants such as grapes, peanuts, and blueberries (Chen et al. 2002). RSV has a large number of biological actions including antioxidative stress (Queiroz et al. 2009), anti-inflammation (Sanchez-Fidalgo et al. 2010), and anticarcinogenic activities (Zykova et al. 2008) as well as neuroprotective effects (Sonmez et al. 2007). The capability of RSV to alleviate oxidative stress and mitochondrial dysfunction in models of PD has been reported (Jin et al. 2008; Zeng et al. 2017) and found to be a neuroprotective agent in both in vitro and in vivo models of neurodegenerative diseases (Kairisalo et al. 2011).

Despite its potential health benefits in humans, RSV is practically water insoluble and has slow dissolution rate resulting in poor oral bioavailability (Hao et al. 2015). Hence, clinical application of this drug greatly restricted. In this regard, several strategies have been developed to circumvent this problem, including nanoparticles. According to the Noyes and Whitney equation, particle size reduction effectively increases the surface area of poorly water-soluble compounds and therefore enhances the solubility and dissolution rate (Dokoumetzidis and Macheras 2006). The reduction of particle size of the RSV is one of the excellent drug delivery system which enhances the saturation solubility and dissolution rate.

The present study aimed to examine resveratrol nanoparticles (NRSV) as a new delivery system for the treatment of PD. Here, we prepared NRSV by antisolvent precipitation method using syringe pump; NRSV were then characterized for their particle size and morphology, and further, the neuroprotective efficacy of NRSV was compared with that of free RSV in an experimental model of rotenone-induced neurodegeneration in rats.

Materials and methods

Materials

Rotenone, resveratrol, glutathione, 5,5-dithiobis[2-nitrobenzoic acid] (DTNB), coenzyme Q, and NADH were purchased from Sigma-Aldrich (USA), the absolute ethanol (99.5–99.8%) was obtained from Merck, Mumbai, India. All other reagents used were also of analytical grade.

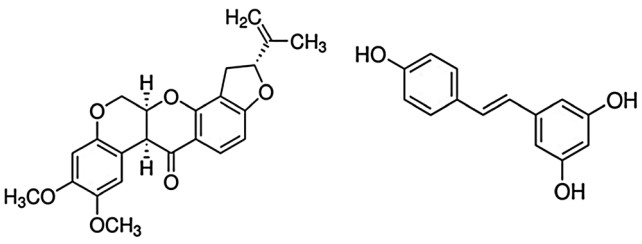

Rotenone
$C_{23}H_{22}O_6$

Resveratrol
$C_{14}H_{12}O_3$

Fig. 1 Chemical structures of rotenone and resveratrol

Preparation of NRSV

The NRSV were prepared by temperature-controlled antisolvent precipitation method using syringe pump (Kim et al. 2012). RSV was dissolved in the solvent ethanol and prepared a solution at a predetermined concentration of 60 mg/mL. The obtained organic solution was added to precooled (5 °C) antisolvent (deionized water) in a dropwise manner under rapid magnetic stirring at 1000 rpm. The formed NRSV were filtered and vacuum dried.

Particle morphology

The particle size and morphology of samples were observed using a scanning electron microscope (SEM) Zeiss EVO 18-EDX special edition machine compatible with EDX machine. The powder samples were spread on a SEM stub and sputtered with gold before the SEM observations. The particle size and texture of nanoparticles can be analyzed by using image magnification software compatible with SEM and helps in determining the presence and formation of NRSV. Five SEM pictures were used to find the average range of particle diameter.

In vitro dissolution testing

The in vitro dissolution of the prepared NRSV samples, as well as the original RSV, was determined using the paddle method (USP 29 type II) (Electro Lab, TDT 06P) in 100 mL of simulated intestinal fluid (SIF, pH 6.8). The rotation speed of paddle was set at 100 rpm, and the bath temperature was kept at 37 ± 0.5 °C. The original RSV and NRSV containing 5 mg of sample were tested for their dissolution in simulated intestinal fluid (Shantha and Harding 2000). Samples of 1 mL volume were collected at 15, 30, 45, 60, 90, 120, and 180 min of dissolution time. The dissolution test for each sample was performed in triplicate, and the dissolution data was averaged. The absorbance was measured at 308 nm using UV spectrometer.

Animals

Male albino Wistar rats (180–250 g) were purchased from Mahaveera Enterprises, Hyderabad. The rats were kept in polyacrylic cages and maintained under standard laboratory conditions (room temperature 24–27 °C and humidity 60–65%). Each experimental group consisted of six animals that were chosen randomly from different cages. Handling and experimentation were conducted in accordance with the approved guidelines of the Committee for the Purpose of Control and Supervision of Experiments on Animals

(CPCSEA), New Delhi, and the experimental protocol was approved by Institutional Animal Ethical Committee (IAEC), Kakatiya University, Warangal.

Treatments

Animals were randomly assigned into four different groups ($n = 12$) as follows: group I received sunflower oil (1 mL/kg s.c.) and served as control, while group II animals were administered with rotenone at a dose of 2 mg/kg s.c. (emulsified in sunflower oil at 2 mg/mL) for a period of 35 days (Verma and Nehru 2009). Group III animals received RSV (40 mg/kg, p.o.) for 35 days; group IV animals were administered NRSV (40 mg/kg, p.o.) for 35 days. Groups III and IV dosed once in a day with rotenone (2 mg/kg, s.c.) along with the respective drugs for a period of 35 days.

Behavioral quantification was done after 24 h of the last dose and before the sacrifice of animals. Animals were randomly divided for the biochemical studies, histological analysis, and neurochemical studies.

Behavioral experiments

Rearing behavior

The test was carried out to assess rearing activity; animals were placed in a clear plexiglas cylinder (height = 30 cm, diameter = 20 cm) for 5 min, and the number of rears was quantified. The rear was classified, when the animal raised his forelimbs above shoulder level, and make contact with the cylinder wall with either one or both forelimbs. Removal of both forelimbs from the cylinder wall and contact with the table surface was required before another rear was scored (Tapias et al. 2014).

Rota rod test

Motor incoordination and grip strength were assessed by rota rod apparatus (Instruments and Chemicals, Ambala, New Delhi). The rota rod consists of horizontal stainless steel rod, 6 cm in diameter and 36 cm long, with a non-slippery surface 20 cm above the base (trip plate). In the present study, the accelerating rotor mode was used (from 2 to 20 rpm). Animals were placed on the rotating rod with its head opposite to the direction of the movement of the rod. The cutoff time was 180 s. A trial was stopped when the rat fell off the rota rod or after the complete 180 s. Three separate trials after 5-min gap were given to each rat. Average of the three trials was taken as the motor coordination index (Banji et al. 2013).

Isolation of brain and preparation of mitochondrial fraction

In order to determine biochemical markers, at the end of the experiment, animals were euthanized and perfused with normal saline solution (37 °C). The perfused brains were immediately removed, and the midbrain tissue of each animal was used for isolation of mitochondrial fractions as described earlier (Moreadith and Fiskum 1984) with minor modifications. Briefly, 10% *w*/*v* homogenate of the brain was prepared in ice-cold homogenizing solution (Tris–sucrose buffer, 0.25 M, pH 7.4) for 1 min. Homogenization was performed with 10–12 strokes set to 600–1000 rpm at 4 °C. The homogenate was then inspected; if intact tissue was still evident, the homogenization was repeated. Resulting homogenates were centrifuged at 1000×*g* for 10 min at 4 °C to obtain the nuclear pellet. Mitochondria were obtained by centrifuging the post-nuclear supernatant at 10,000×*g* for 20 min at 4 °C to obtain the mitochondrial pellet and cytosolic fraction. The mitochondrial pellet obtained was washed with the same medium to obtain the mitochondrial preparation which was used for the estimations.

Tricarboxylic acid cycle enzymes

Succinate dehydrogenase

Succinate dehydrogenase activity was assessed according to the method of King et al. (1976). This assay is based on oxidation of succinate to fumarate by an artificial electron acceptor, potassium ferricyanide, catalyzed by enzyme succinate dehydrogenase. In this procedure, the reaction was initiated by addition of a requisite amount of mitochondrial sample to the reaction mixture containing 0.2 M sodium phosphate buffer (pH 7.8), 1% (*w*/*v*) bovine serum albumin, 0.6 M sodium succinate, and 0.03 M potassium ferricyanide. The change in absorbance was read at 420 nm for 3 min. The concentration of succinate dehydrogenase was expressed as nanomoles of succinate oxidized per minute per milligram protein using molar extinction coefficient (1000 M^{-1} cm^{-1}).

Aconitase

Aconitase was assayed as described by Racker (1950). To 50 μL of 1/5 diluted mitochondrial suspension, 100 mM Tris buffer (pH 8) and 50 mM citrate were added up to 1 mL and absorbance was read at 240 nm. The concentration of aconitase was calculated using molar extinction coefficient of 3.6 mM^{-1} cm^{-1}, and the result was expressed as nanomoles of cis-aconitase formed per minute per milligram protein.

Citrate synthase

Citrate synthase content was measured according to the method of Srere (1969). To 50 μL of 1/5 diluted mitochondrial fraction, 0.1 mM acetyl coenzyme A, 0.2 mM dithionitrobenzoic acid, and 100 mM Tris HCl (pH 8) were added. Finally, 0.2 mM oxaloacetate was added to the above mixture, and the absorbance was read at 412 nm for 3 min with 15-s interval. The concentration of citrate synthase was calculated using molar extinction coefficient of 13.6 mM^{-1} cm^{-1}, and the result was expressed as nanomoles of dinitrobenzoic acid formed per minute per milligram protein.

Complex-I activity

Complex-I activity was measured as described by Hatefi and Rieske (1967). To 50 μL of mitochondrial fraction, 880 μL of double distilled water, 50 μL of 1 M phosphate buffer (pH 8), 50 μL of 1 M coenzyme Q (CoQ), and 12 μL of 10 mM NADH were added. Absorbance was read at 340 nm for 3 min at 15-s interval. The concentration of complex I was calculated by using molar extinction coefficient of 6.3 mM^{-1} cm^{-1}, and the specific enzyme activity was expressed as nanomoles of NADH oxidized per minute per millligram protein.

Oxidative parameters

Estimation of lipid peroxidation was carried out according to the method of Ruiz-Larrea et al. (1994). This assay involves the reaction of malondialdehyde (MDA) equivalents with thiobarbituric acid (TBA) to yield a pink complex. The absorbance was measured at 532 nm, and MDA brain content was expressed as nanomole per milligram tissue. GSH activity was assayed spectrophotometrically by the method of Ellman (1959) and Bulaj et al. (1998). The optical density of the produced colored product was determined at 412 nm. Calculation of glutathione (GSH) content was based on a standard glutathione curve, and the level was expressed as micromole per milligram tissue. Catalase activity was assayed spectrophotometrically by the method of Beer and Seizer (1951) based on the ability of catalase to oxidize hydrogen peroxide. The change in absorbance was read at 240 nm. The enzymatic activity was expressed as nanomoles of H_2O_2 decomposed per minute per milligram protein.

Histopathology

The brain sections were fixed in freshly prepared 10% neutral buffered formalin, processed routinely, and embedded in paraffin. In addition, 4-μm-thick paraffin sections were prepared and stained with hematoxylin and eosin (H&E) for histopathological examination. Sections were examined using a light microscope.

Statistical analysis

The mean ± SEM were calculated for all data. Significant difference between means was evaluated by one-way analysis of variance (ANOVA) followed by Bonferroni multiple comparison tests. $p < 0.05$ was considered as statistically significant.

Results

NRSV characterization by SEM

SEM micrographs of the RSV and NRSV are shown in Fig. 2a, b. It is observed that the RSV powder (Fig. 2a) exhibited particles lacking uniformity in size and were much larger than the NRSV (Fig. 2b). On the other hand, NRSV prepared by syringe pump exhibited particle uniformity in size, less crystallinity, and absence of larger particles (Fig. 2b). As depicted in the image, the particles possessed uniform shape. The size of all particles was found to be within the range of 50–200 nm.

In vitro dissolution

The dissolution profiles of the commercial RSV and the formulated NRSV in simulated intestinal fluid (SIF, pH 6.8) are shown in Fig. 3. NRSV were dissolved 85% at 90 min. On the other hand, 48% of the commercial RSV was dissolved in the same period. It was observed that NRSV reached 50% dissolution in 30 min. Whereas the commercial RSV did not reach even 50% dissolution within 90 min.

Behavioral experiments

Rearing behavior

Administration of rotenone significantly decreased the number of rears ($p < 0.05$) as compared to the control animals. Treatment with RSV and NRSV increased the rearing counts when compared to rotenone-treated animals. NRSV treatment significantly reversed ($p < 0.05$) the rotenone-induced changes in rearing behavior (Fig. 4).

Rota rod test

Rotenone treatment significantly decreased the latency to fall down from the rota rod compared to the control ($p < 0.05$). Treatment with RSV and NRSV produced an increase in latency to fall down compared to the rotenone-treated group. NRSV treatment significantly enhanced the latency to fall down from the rota rod compared to the rotenone-treated group ($p < 0.05$) (Fig. 5).

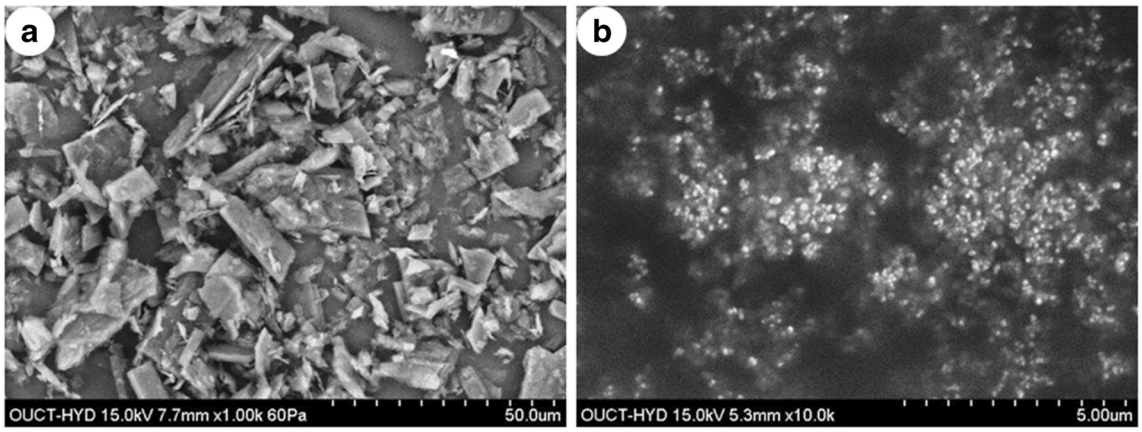

Fig. 2 SEM photographs of (**a**) RSV and (**b**) NRSV

Assessment of TCA enzymes

Succinate dehydrogenase, citrate synthase, and aconitase activities significantly decreased in the rotenone-treated group (18.666 ± 0.8986, 9.607 ± 0.4625, 10.888 ± 0.5242) as compared to control group ($p < 0.05$). Treatment with RSV was effective in raising the levels of succinate dehydrogenase, citrate synthase, and aconitase compared to rotenone-treated group. NRSV treatment significantly ($p < 0.05$) restored the levels of succinate dehydrogenase, citrate synthase, and aconitase (30.761 ± 0.5409, 15.833 ± 0.2784, 17.944 ± 0.3155) compared to rotenone-treated group (Table 1).

Estimation of complex-I activity

Rotenone treatment significantly ($p < 0.05$) decreased the activity of the mitochondrial complex-I (27.1692 ± 0.3901) as compared to the control group. RSV treatment increased the activity of complex-I compared to rotenone-treated group. The activity of complex-I significantly ($p < 0.05$) restored in NRSV-treated group (24.3 ± 0.3908) as compared to rotenone-treated group (Table 1).

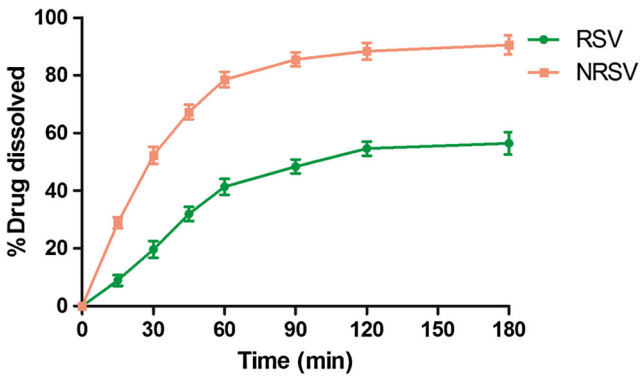

Fig. 3 Dissolution profile of commercial RSV and NRSV

Determination of lipid peroxidation

Animals subjected to rotenone treatment showed a significant ($p < 0.05$) increase in LPO which is measured as MDA levels (3.833 ± 0.1621) as compared to control group. NRSV treatment showed a significant decrease ($p < 0.05$) in brain MDA levels (1.167 ± 0.3326) compared to rotenone group. RSV did not show the significant increase in MDA levels compared to rotenone group (Table 2).

GSH activity

Decreased levels of GSH (0.888 ± 0.1275) were observed in animals treated with rotenone as compared to control group. Treatment with RSV has shown declined levels of GSH compared to rotenone-treated group. NRSV treatment of animals significantly ($p < 0.05$) restored the levels of GSH (3.032 ± 0.0753) compared to rotenone group (Table 2).

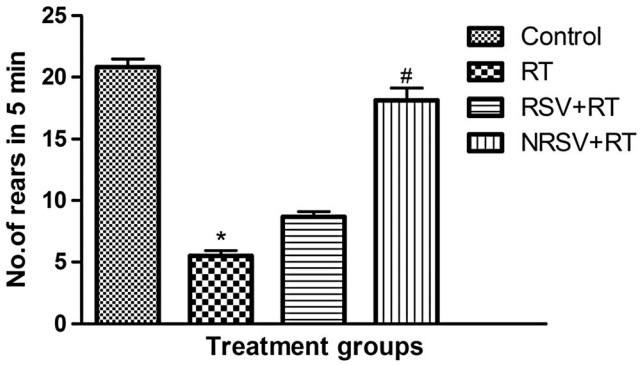

Fig. 4 Effects of NRSV (40 mg/kg, p.o.), RSV (40 mg/kg, p.o.), and rotenone (RT) (2 mg/kg, s.c.) on rearing behavior in rats. Each bar with vertical line represented as mean values ± SEM. Statistical analysis was carried out using one-way ANOVA followed by Bonferroni multiple comparison test; $^{\#}p < 0.05$ vs. rotenone; $^{*}p < 0.05$ vs. control

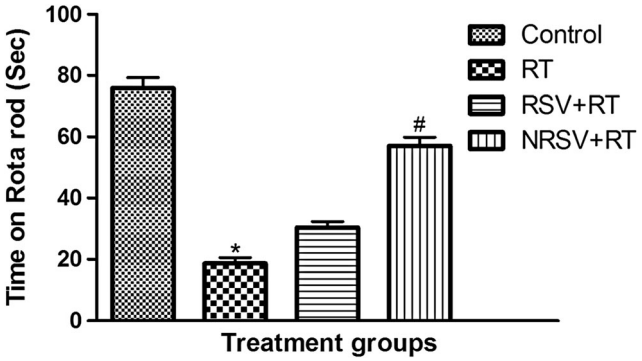

Fig. 5 Effects of NRSV (40 mg/kg, p.o.) and RSV (40 mg/kg, p.o.) on rotenone (RT) (2 mg/kg, s.c.) induced motor deficits in rota rod test. Each bar with vertical line represented as mean values ± SEM. Statistical analysis was carried out using one-way ANOVA followed by Bonferroni multiple comparison test; $^{\#}p < 0.05$ vs. rotenone; $^{*}p < 0.05$ vs. control

Catalase activity

Table 2 depicts the effect of different treatments on catalase. The catalase levels were significantly ($p < 0.05$) decreased in rotenone-treated rats (2.50 ± 0.3055) as compared to control group. Treatment with RSV raised the levels of catalase compared to rotenone group. Significant increase ($p < 0.05$) in catalase levels was observed in NRSV group (7.367 ± 0.2716) as compared to rotenone-treated group (Table 2).

Histopathological studies

Histological features of hematoxylin and eosin-stained sections from the substantia nigra of rats are depicted in Fig. 6. (a) Sections from the control group exhibited normal neuronal structure that showed dispersed chromatin and prominent nucleoli. (b) Sections from the rotenone-treated rats showed marked neuronal degeneration, pyknotic darkly stained nuclei, cellular accumulation, and chromatolysis. (c) RSV was weaker in preventing the neuronal alterations induced by rotenone. (d) NRSV treatment prevented the degenerative alterations caused by rotenone and showed nearly normal morphological appearance with mild pyknotic darkly stained nuclei and cellular accumulation.

Discussion

Nanoparticles have potentially been used for the treatment of various neurodegenerative diseases (Spuch et al. 2012). In the present study, the NRSV was successfully prepared by temperature-controlled antisolvent precipitation method to decrease the particle size and to enhance the water solubility of RSV. The SEM analysis of NRSV revealed that the formation of nanoparticles showed the spherical shape and found to be within the range of 50–200 nm. In addition to that, in vitro dissolution study of NRSV has shown high dissolution rate as compared to the commercial RSV. It was reported that particle size reduction of a poorly water-soluble compound to nanoparticles results in the formation of a thinner hydrodynamic layer around particles and increases the surface specific dissolution rate (Mosharrafand and Nystrom 1995; Kesisoglou et al. 2007). Here, we can conclude that the higher dissolution rate of NRSV resulted from the decreased particle size and could translate into increased bioavailability.

Several studies have demonstrated the neuroprotective effects of RSV in both in vitro and in vivo models (Sonmez et al. 2007). RSV enhances various antioxidant enzymes in the brains of healthy rats and exerts potential antioxidant effects by crossing the blood-brain barrier (Mokni et al. 2007). Lu et al. (2013) reported that nanoparticles of RSV showed a potent neuroprotective effect in a model of oxidative stress induced by hydrogen peroxide in cortical cell culture than free drug. Neuroprotective effects of NRSV against rotenone-induced neurotoxicity in rats have not been studied to date, to our knowledge. Hence, the present study was done to evaluate the protective effect of NRSV against rotenone-induced elevated oxidative stress along with associated behavioral, neurochemical, and histopathological changes in a rat model of PD.

Table 1 Effects of NRSV (40 mg/kg, p.o.) and RSV (40 mg/kg, p.o.) on rotenone (RT) (2 mg/kg, s.c.) induced mitochondrial enzyme alterations in rat brain

Treatment groups	Succinate dehydrogenase (μM/min/mg protein)	Citrate synthase (μM/min/mg protein)	Aconitase (μM/min/mg protein)	Complex-I activity (μM/min/mg protein)
I Control	33.404 ± 0.5903	17.193 ± 0.3038	19.486 ± 0.3443	27.1692 ± 0.3901
II RT	18.666 ± 0.8986*	9.607 ± 0.4625*	10.888 ± 0.5242*	14.459 ± 0.7895*
III RSV + RT	23.325 ± 0.5549	11.924 ± 0.3932	12.587 ± 0.3605	16.984 ± 0.5822
IV NRSV + RT	30.761 ± 0.5409**	15.833 ± 0.2784**	17.944 ± 0.3155**	24.3 ± 0.3908**

The results expressed as mean ± SEM, $n = 6$. Statistical analysis was carried out by one-way ANOVA followed by Bonferroni multiple comparison test
$^{*}p < 0.05$ vs. control group; $^{**}p < 0.05$ vs. rotenone group

Table 2 Effects of NRSV (40 mg/kg, p.o.) and RSV (40 mg/kg, p.o.) on rotenone (RT) (2 mg/kg, s.c.) induced oxidative stress parameters in rat brain

Treatment groups	MDA (nmol/mg tissue)	GSH (μmol/mg tissue)	Catalase (nmol/mg tissue)
I Control	0.862 ± 0.1935	3.651 ± 0.2418	8.967 ± 0.1520
II RT	3.833 ± 0.1621*	0.888 ± 0.1275*	2.50 ± 0.3055*
III RSV + RT	2.998 ± 0.2455	1.699 ± 0.1177	3.883 ± 0.5969
IV NRSV + RT	1.167 ± 0.3326**	3.032 ± 0.0753**	7.367 ± 0.2716**

The results expressed as mean ± SEM, $n = 6$. Statistical analysis was carried out by one-way ANOVA followed by Bonferroni multiple comparison test

*$p < 0.05$ vs. control group; **$p < 0.05$ vs. rotenone group

In animal models of PD, chronic rotenone treatment has been widely used for the induction of neurotoxicity, since it has certain advantages for experimental studies as compared to other models (Bezard et al. 2013). Rotenone is a membrane-permeable compound that accumulates in subcellular organelles like mitochondria and causes mitochondrial dysfunction which leads to increased oxidative stress (Uversky 2004).

Rota rod test has been widely used to identify deficits in the motor coordination of rodent PD models (von Wrangel et al. 2015). In this study, rotenone-treated rats have shown significant decreases in the latency to fall down from the rota rod as compared to control. On the other hand, NRSV provided significant functional recovery of the retention time on the rota rod as compared to RSV. In rearing test, decreased rearing counts observed in rotenone-treated group as compared to control group. Animals treated with NRSV have shown more consistent increase in rearing counts when compared to animals in the RSV group. In both the behavioral experiments, NRSV and RSV treatments reversed the changes in rearing counts and grip strength due to rotenone treatment. These effects were observed maximum in group treated with NRSV, which were comparable to the control group. The improved behavioral response in the NRSV group is due to high potential for improving the oral bioavailability of nanoparticles.

Mitochondrial enzymes generate ATP through the two metabolic pathways. The first one is tricarboxylic acid (TCA) cycle, and the other one is mitochondrial electron transport chain, thereby maintaining neuronal homeostasis defects in mitochondrial function has led to the conception that the mitochondrion is responsible for several neurodegenerative disorders including PD (Mizuno et al. 1998; Schapira et al. 1990). Complex-I is a major component of electron transport chain, the loss of which triggers the generation of free radicals (Cai et al. 1998). Chronic administration of rotenone at low doses detrimentally affects TCA enzymes and also decreases complex-I activity which could contribute to increase in oxidative stress (Tapias et al. 2014). RSV and NRSV treatments to rotenone

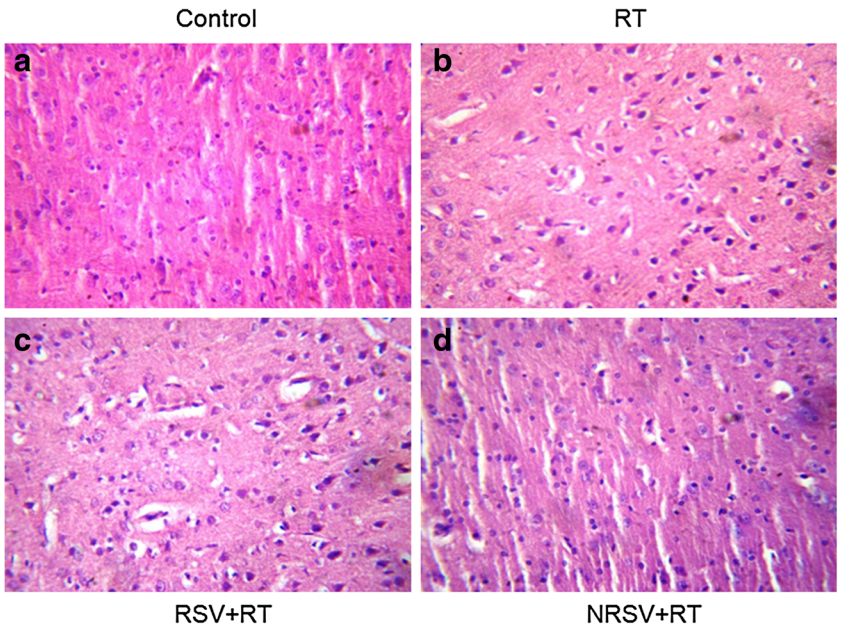

Fig. 6 Hematoxylin and eosin (H&E) stained photomicrographs of the substantia nigra from each studied group. **a** Control: normal morphology of brain tissue. **b** Rotenone (RT): pyknotic darkly stained nuclei, cellular accumulation, and chromatolysis. **c** Resveratrol (RSV) + RT: mild pyknotic darkly stained nuclei and cellular accumulation. **d** Resveratrol nanoparticles (NRSV) + RT: nearly normal morphological appearance of with fewer pyknotic darkly stained nuclei

animals significantly restored the activities of complex-I and TCA enzymes. These findings are in agreement with the recent reports which showed that resveratrol attenuates oxidative stress in mitochondrial dysfunction (Mathieu et al. 2016; Weijun Zeng et al. 2017). NRSV administration significantly improved the activity of both complex-I and TCA enzymes as compared to RSV implying that it might be due to improved efficacy.

Early studies reported that impaired mitochondrial complex-I activity leads to the generation of free radicals and increased oxidative stress (Kudin et al. 2004). In this study, LPO levels were found to be elevated and antioxidant enzymes like catalase and GSH were found to be decreased in the brains of rotenone-treated animals suggesting an increase in oxidative stress. NRSV treatment significantly restored the antioxidant enzymes and decreased the LPO levels as compared to the RSV.

The hypothesis behind the more pronounced pharmacological effects of NRSV than RSV is the use of nanoparticles. In the animal models of many neurodegenerative disorders, several studies have reported that there is a clear inverse correlation among nanoparticle size of the therapeutic drug and blood-brain barrier (BBB) penetration (Hanada et al. 2014; Saraiva et al. 2016). Here, we demonstrated the use of NRSV as an alternative to the RSV treatment and its nanodelivery is a promising tool in the therapeutic application of PD. Additional investigations are already in progress to determine the bioavailability of NRSV in the central nervous system.

Conclusion

It can be concluded from our study that formulated NRSV could maintain RSV blood levels for a longer time, increasing its bioavailability and, therefore, its pharmacological effect. Hence, the NRSV showed comparatively better efficacy in attenuating the rotenone-induced PD-like behavioral alterations, biochemical and histological changes, oxidative stress, and mitochondrial dysfunction in rats than the RSV treatment. Therefore, this approach of nanoparticles may open new perspectives for the treatment of neurodegenerative diseases in the future if it is extrapolated to the human studies.

Acknowledgments University College of Pharmaceutical Sciences, Kakatiya University, support for the routine reagents and permission to animal holding for this research.

Compliance with ethical standards

Conflict of interest The authors declare that they have no conflict of interest.

References

Alam M, Schmidt WJ (2002) Rotenone destroys dopaminergic neurons and induces parkinsonian symptoms in rats. Behav Brain Res 136(1):317–324. https://doi.org/10.1016/S0166-4328(02)00180-8

Banji D, Banji OJ, Dasaroju S, Kranthi KC (2013) Curcumin and piperine abrogate lipid and protein oxidation induced by D-galactose in rat brain. Brain Res 1515:1–11. https://doi.org/10.1016/j.brainres.2013.03.023

Beer RF, Seizer TW (1951) A spectrophotometric method for measuring breakdown of hydrogen peroxide by catalase. J Biol Chem 115: 130–140

Betarbet R, Sherer TB, MacKenzie G, Garcia-Osuna M, Panov AV, Greenamyre JT (2000) Chronic systemic pesticide exposure reproduces features of Parkinson's disease. Nat Neurosci 3(12):1301–1306. https://doi.org/10.1038/81834

Bezard E, Yue Z, Kirik D, Spillantini MG (2013) Animal models of Parkinson's disease limits and relevance to neuroprotection studies. Mov Disord 28(1):61–70. https://doi.org/10.1002/mds.25108

Bueler H (2009) Impaired mitochondrial dynamics and function in the pathogenesis of Parkinson's disease. Exp Neurol 218(2):235–246. https://doi.org/10.1016/j.expneurol.2009.03.006

Bulaj G, Kortemme T, Goldenberg DP (1998) Ionization-reactivity relationships for cysteine thiols in polypeptides. Biochemistry 37:8965–8972

Cai J, Yang J, Jones DP (1998) Mitochondrial control of apoptosis: the role of cytochrome c. Biochim Biophys Acta 1366:139–149

Chen RS, Wu PL, Chiou RYY (2002) Peanut roots as a source of resveratrol. J Agric Food Chem 50(6):1665–1667. https://doi.org/10.1021/jf011134e

Dokoumetzidis A, Macheras P (2006) A century of dissolution research: from Noyes and Whitney to the biopharmaceutics classification system. Int J Pharm 321(1-2):1–11. https://doi.org/10.1016/j.ijpharm.2006.07.011

Ellman GL (1959) Tissue sulfhydryl groups. Arch Biochem Biophys 82(1):70–77. https://doi.org/10.1016/0003-9861(59)90090-6

Hanada S, Fujioka K, Inoue Y, Kanaya F, Manome Y, Yamamoto K (2014) Cell-based in vitro blood–brain barrier model can rapidly evaluate nanoparticles' brain permeability in association with particle size and surface modification. Int J Mol Sci 15(2):1812–1825. https://doi.org/10.3390/ijms15021812

Hao J, Gao Y, Zhao J, Zhang J, Li Q, Zhao Z, Liu J (2015) Preparation and optimization of resveratrol nanosuspensions by antisolvent precipitation using Box-Behnken design. AAPS PharmSciTech 16: 118–128

Hatefi Y, Rieske JS (1967) Preparation and properties of DPNH-coenzyme Q reductase (complex I of the respiratory chain). Methods Enzymol 10:235–239. https://doi.org/10.1016/0076-6879(67)10046-3

Hu LF, Lu M, Tiong CX, Dawe GS, Hu G, Bian JS (2010) Neuroprotective effects of hydrogen sulfide on Parkinson's disease rat models. Aging Cell 9(2):135–146. https://doi.org/10.1111/j.1474-9726.2009.00543.x

Jin F, Wu Q, Lu YF, Gong QH, Shi JS (2008) Neuroprotective effect of resveratrol on 6-OHDA-induced Parkinson's disease in rats. Eur J Pharmacol 600(1-3):78–82. https://doi.org/10.1016/j.ejphar.2008.10.005

Kairisalo M, Bonomo A, Hyrskyluoto A, Mudò G, Belluardo N, Korhonen L, Lindholm D (2011) Resveratrol reduces oxidative stress and cell death and increases mitochondrial antioxidants and XIAP in PC6.3-cells. Neurosci Lett 488:263–266

Kesisoglou F, Panmai S, Wu Y (2007) Nanosizing-oral formulation development and biopharmaceutical evaluation. Adv Drug Deliv Rev 59(7):631–644. https://doi.org/10.1016/j.addr.2007.05.003

Khurana N, Gajbhiye A (2013) Ameliorative effect of Sida cordifolia in rotenone induced oxidative stress model of Parkinson's disease. Neurotoxicology 39:57–64. https://doi.org/10.1016/j.neuro.2013.08.005

Kim S, Ng WK, Dong Y, Das S, Tan RBH (2012) Preparation and physicochemical characterization of trans-resveratrol nanoparticles by temperature-controlled antisolvent precipitation. J Food Eng 108(1):37–42. https://doi.org/10.1016/j.jfoodeng.2011.07.034

King TE, Ohnishi T, Winter DB, Wu JT (1976) Biochemical and EPR probes for structure–function studies of iron sulfur centers of succinate dehydrogenase. Adv Exp Med Biol 74:182–227. https://doi.org/10.1007/978-1-4684-3270-1_15

Kudin AP, Bimpong-Buta NY, Vielhaber S, Elger CE, Kunz WS (2004) Characterization of superoxide-producing sites in isolated brain mitochondria. J Biol Chem 279(6):4127–4135. https://doi.org/10.1074/jbc.M310341200

Lu X, Xu H, Sun B, Zhu Z, Zheng D, Li X (2013) Enhanced neuroprotective effects of resveratrol delivered by nanoparticles on hydrogen peroxide-induced oxidative stress in rat cortical cell culture. Mol Pharm 10(5):2045–2053. https://doi.org/10.1021/mp400056c

Mathieu L, Costa AL, Le Bachelier C, Slama A, Lebre AS, Taylor RW, Bastin J, Djouadi F (2016) Resveratrol attenuates oxidative stress in mitochondrial complex I deficiency: involvement of SIRT3. Free Radic Biol Med 96:190–198. https://doi.org/10.1016/j.freeradbiomed.2016.04.027

Mizuno Y, Yoshino H, Ikebe S, Hattori N, Kobayashi T, Shimoda-Matsubayashi S, Matsumine H, Kondo T (1998) Mitochondrial dysfunction in Parkinson's disease. Ann Neurol 44:99–109

Mokni M, Elkahoui S, Limam F, Amri M, Aouani E (2007) Effect of resveratrol on antioxidant enzyme activities in the brain of healthy rat. Neurochem Res 32:981–987

Moreadith RW, Fiskum G (1984) Isolation of mitochondria from ascites tumor cells permeabilized with digitonin. Anal Biochem 137(2):360–367. https://doi.org/10.1016/0003-2697(84)90098-8

Mosharrafand M, Nystrom C (1995) The effect of particle size and shape on the surface specific dissolution rate of microsized practically insoluble drugs. Int J Pharm 122(1-2):35–47. https://doi.org/10.1016/0378-5173(95)00033-F

Olanow CW, Agid Y, Mizuno Y et al (2004) Levodopa in the treatment of Parkinson's disease: current controversies. Mov Disord 19(9):997–1005

Queiroz AN, Gomes BA, Moraes WM, Borges RS (2009) A theoretical antioxidant pharmacophore for resveratrol. Eur J Med Chem 44(4):1644–1649. https://doi.org/10.1016/j.ejmech.2008.09.023

Racker E (1950) Spectrophotometric measurement of the enzymatic formation of fumaric and cis-aconitic acids. Biochim Biophys Acta 4(1-3):211–214. https://doi.org/10.1016/0006-3002(50)90026-6

Ruiz-Larrea MB, Leal AM, Liza M, Lacort M, de Groot H (1994) Antioxidant effects of estradiol and 2-hydroxyestradiol on iron induced lipid peroxidation of rat liver microsomes. Steroids 59(6):383–388

Sanchez-Fidalgo S, Cardeno A, Villegas I, Talero E, de la Lastra CA (2010) Dietary supplementation of resveratrol attenuates chronic colonic inflammation in mice. Eur J Pharmacol 633:78–84

Saraiva C, Praça C, Ferreira R, Santos T, Ferreira L, Bernardino L (2016) Nanoparticle-mediated brain drug delivery: overcoming blood–brain barrier to treat neurodegenerative diseases. J Control Release 235:34–47. https://doi.org/10.1016/j.jconrel.2016.05.044

Saravanan KS, Sindhu KM, Mohanakumar KP (2005) Acute intranigral infusion of rotenone in rats causes progressive biochemical lesions in the striatum similar to Parkinson's disease. Brain Res 1049(2):147–155. https://doi.org/10.1016/j.brainres.2005.04.051

Schapira AH, Copper JM, Clark JB, Jenner P, Marsden CD (1990) Mitochondrial complex-I deficiency in Parkinson's disease. J Neurochem 54(3):823–827. https://doi.org/10.1111/j.1471-4159.1990.tb02325.x

Shantha KL, Harding DRK (2000) Preparation and in vitro evaluation of poly (Nvinyl-2-pyrrolidone-polyethylene glycol diacrylate)-chitosan interpolymeric pH responsive hydrogels for oral drug delivery. Int J Pharm 207(1-2):65–70. https://doi.org/10.1016/S0378-5173(00)00533-0

Sonmez U, Sonmez A, Erbil G, Tekmen I, Baykara B (2007) Neuroprotective effects of resveratrol against traumatic brain injury in immature rats. Neurosci Lett 420:133–137

Spuch C, Saida O, Navarro C (2012) Advances in the treatment of neurodegenerative disorders employing nanoparticles. Recent Pat Drug Deliv Formul 6(1):2–18

Srere PA (1969) Citrate synthase. In: Lowenstein JM (ed) Methods in enzymology, citric acid cycle. Academic, New York, pp 3–11. https://doi.org/10.1016/0076-6879(69)13005-0

Swarnkar S, Singh S, Sharma S, Mathur R, Patro IK, Nath C (2011) Rotenone induced neurotoxicity in rat brain areas: a histopathological study. Neurosci Lett 501(3):123–127. https://doi.org/10.1016/j.neulet.2011.03.036

Tapias V, Cannon JR, Greenamyre JT (2014) Pomegranate juice exacerbates oxidative stress and nigrostriatal degeneration in Parkinson's disease. Neurobiol Aging 35(5):1162–1176. https://doi.org/10.1016/j.neurobiolaging.2013.10.077

Uversky VN (2004) Neurotoxicant induced animal models of Parkinson's disease: understanding the role of rotenone, maneb and paraquat in neurodegeneration. Cell Tissue Res 318(1):225–241. https://doi.org/10.1007/s00441-004-0937-z

Verma R, Nehru B (2009) Effect of centrophenoxine against rotenone induced oxidative stress in an animal model of Parkinson's disease. Neurochem Int 55(6):369–375. https://doi.org/10.1016/j.neuint.2009.04.001

Wang H, Liu J, Gao G, Wu X, Wang X, Yang H (2016) Protection effect of piperine and piperlonguminine from Piper longum L. alkaloids against rotenone-induced neuronal injury. Brain Res 1639:214–227. https://doi.org/10.1016/j.brainres.2015.07.029

von Wrangel C, Schwabe K, John N, Krauss JK, Alam M (2015) The rotenone-induced rat model of Parkinson's disease: behavioral and electrophysiological findings. Behav Brain Res 279:52–61. https://doi.org/10.1016/j.bbr.2014.11.002

Zeng W, Zhang W, Lu F, Gao L, Gao G (2017) Resveratrol attenuates MPP+-induced mitochondrial dysfunction and cell apoptosis via AKT/GSK-3β pathway in SN4741 cells. Neurosci Lett 637:50–56. https://doi.org/10.1016/j.neulet.2016.11.054

Zykova TA, Zhu F, Zhai X, Ma WY, Ermakova SP, Lee KW, Bode AM, Dong Z (2008) Resveratrol directly targets COX-2 to inhibit carcinogenesis. Mol Carcinog 47(10):797–805. https://doi.org/10.1002/mc.20437